Dichotomy between the nodal and antinodal excitations in high-temperature superconductors

Henry Fu and Dung-Hai Lee
Department of Physics, University of California at Berkeley, Berkeley, California 94720, USA
and Material Science Division, Lawrence Berkeley National Laboratory, Berkeley, California 94720, USA
(Received 30 March 2006; published 16 November 2006)

Angle-resolved photoemission data on optimally doped and underdoped high-temperature superconductors reveal a dichotomy between the nodal and antinodal electronic excitations. We propose an explanation of this unusual phenomenon by employing the coupling between the quasiparticle and the commensurate and incommensurate magnetic excitations.

DOI: 10.1103/PhysRevB.74.174513 PACS number(s): 74.72.−h

INTRODUCTION

Angle-resolved photoemission spectroscopy[1] has made important contributions to the understanding of high-temperature superconductors. The information revealed by this technique has pointed to an unusual dichotomy[2] between nodal and antinodal electronic excitations. In particular, as the Mott insulating state at low doping is approached, the quasiparticle weight vanishes on part of the Fermi surface (the antinodal region) while it remains finite on the rest (the nodal region). This is schematically illustrated in Fig. 1. We refer to this strong momentum dependence of the quasiparticle weight as the dichotomy between the nodal and antinodal excitations.

In the rest of the paper we first describe the experimental evidence from ARPES leading to this characterization of the nodal-antinodal dichotomy. Following that we propose a mechanism for the origin of this phenomenon.

NODAL-ANTINODAL DICHOTOMY IN ARPES

Figure 2 illustrates the node→antinode ARPES spectra for $La_{2-x}Sr_xCuO_4$ (LSCO) at a fixed temperature ~20 K of Zhou *et al.*[2] The doping levels for the three panels are 0.063, 0.09, and 0.22 from left to right. For the $x=0.22$ (overdoped) sample a quasiparticle peak is observed at all points on the Fermi surface. In contrast, at $x=0.063$ the quasiparticle peak only exists within a fixed angular range around the node. Similar nodal quasiparticle peaks are observed in even 3%-doped samples.[3]

It should be noted that although the nodal quasiparticle peak exists for all doping, its spectral weight does diminish as $x\to 0$ (see Fig. 3).[4] This diminishing of the quasiparticle weight is well described by a class of theories based on using the Gutzwiller-projected wave function to describe the strongly correlated electronic states.[5] However, these theories do not explain the interesting fact that while nodal excitations are well-defined quasiparticles, antinodal excitations are completely decoherent.

MECHANISM FOR THE ANTINODAL DECOHERENCE

Here we propose a mechanism for the antinodal decoherence that focuses on the role of magnetic excitations and their coupling to the antinodal quasiparticles. Before we begin, we present two experimental clues to the origin of antinodal decoherence: the absence of a large leading-edge gap in ARPES measurements of the antinodes and the existence of low-energy spin excitations.

First, a close-up of the leading edge behavior of the ARPES spectra near the antinode (enclosed by the box in Fig. 4) for 6.3%-doped LSCO (Ref. 2) is illustrated in Fig. 4. A close inspection shows that the set back of these leading edges is only about 10 meV. For doping as low as $x=0.063$ such a small gap is very surprising, because from other measurements—e.g., NMR—the pseudogap should increase with underdoping.[6] Hence at $x=0.063$ one would expect a much larger gap. This leading-edge behavior tells us that there are low-energy excitations with the quantum number of a photohole which are not coherent quasiparticles.

Second, it has been well established that in LSCO there exist low-energy spin excitations in the neighborhood of momentum (π,π).[7] For example, at 6% doping, inelastic neutron scattering demonstrates enhanced spectral weight around $(\pi\pm\delta,\pi)$ and $(\pi,\pi\pm\delta)$ for energies as low as 2 meV (see Fig. 5). In the following we propose that the electronic excitations contributing to the leading-edge spectral weight are continuum excitations made up of low-energy spin excitations and quasiparticles near the nodes.

MECHANISM FOR THE ANTINODAL DECOHERENCE

For momenta equal to those of the nodes (dot *A* of Fig. 6), the lowest-energy excitation consistent with the quantum number of a photohole is the zero-energy quasiparticle. As the momentum moves toward the antinode, the quasiparticle gap increases. It is possible that at an intermediate momentum between the node and antinode, the lowest-energy exci-

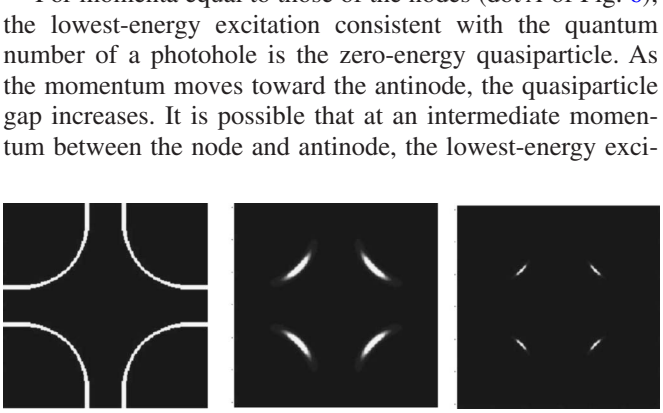

FIG. 1. The Bogoliubov quasiparticle weight z along the normal-state Fermi surface as observed by ARPES. The brightness is proportional to the magnitude of z. The doping decreases from the left to right.

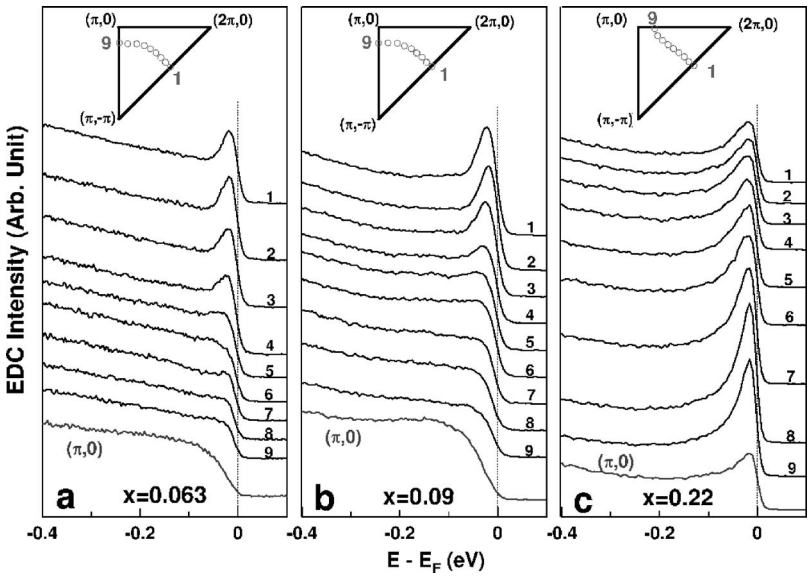

FIG. 2. The nodal (1) to antinodal (9) ARPES spectra for $La_{2-x}Sr_xCuO_4$ at doping $x=0.063, 0.09, 0.22$. From Zhou *et al.* (Ref. 2).

tation ceases to be a quasiparticle. For example, for momentum at the Brillouin zone face (indicated by dot *B* in Fig. 6) a multiparticle excitation with energy lower than the quasiparticle can exist. We propose that this type of multiparticle excitation consists of a quasiparticle with momentum close to the node (dot *C* in Fig. 6) and an incommensurate spin excitation with momentum indicated by the arrow. Such multiparticle excitations contribute to the leading edge of the ARPES spectrum near the antinodes. Since as a function of excitation energy the gapped quasiparticle states are preceded by this multiparticle continuum, they can no longer be coherent. This is because energy conservation allows them to decay into multiparticle states. We note that the origin of the antinodal quasiparticle gap is not important for our mechanism; thus, although we are mainly thinking of the *d*-wave "pseudogap," the charge-density-wave-like scatterings which preferentially affect the antinodes[2,9] can also enhance our mechanism if they open a gap.

Clearly, in order for the above mechanism to work, the spin excitation must cost sufficiently low energy relative to the antinodal gap. If this requirement is not met, antinodal quasiparticle peaks will be exhibited and the leading edge will be determined by the quasiparticle gap. Under such conditions the nodal-antinodal dichotomy is absent. We expect this to happen when the doping is sufficiently high and the antinodal gap becomes smaller than the energy of spin excitations.

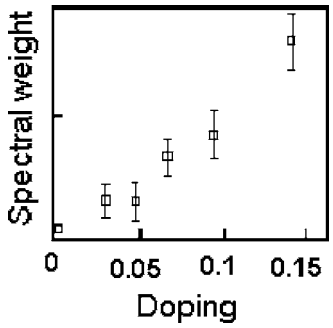

FIG. 3. The spectral weight of the nodal quasiparticle peak as a function of doping. From Shen *et al.* (Ref. 4).

RENORMALIZATION GROUP PERSPECTIVE

Although our mechanism for the antinodal decoherence is proposed on phenomenological grounds, it also finds some support from renormalization group (RG) analyses. Starting from the overdoped side, which is widely believed to be a Fermi liquid, we expect that decreasing doping introduces residual quasiparticle interactions. For doping that is not too low, the effects of these residual interactions can be analyzed in a perturbative RG approach. This point of view has been

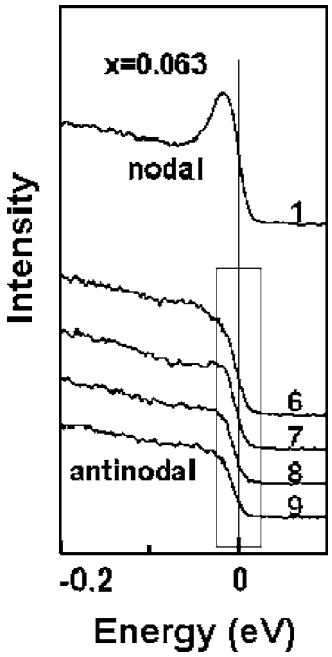

FIG. 4. The set back of the leading edge near the antinode (enclosed by box) is only ≈10 meV. The spectra are taken at momenta labeled as in Fig. 2(a). From Zhou *et al.*(Ref. 2).

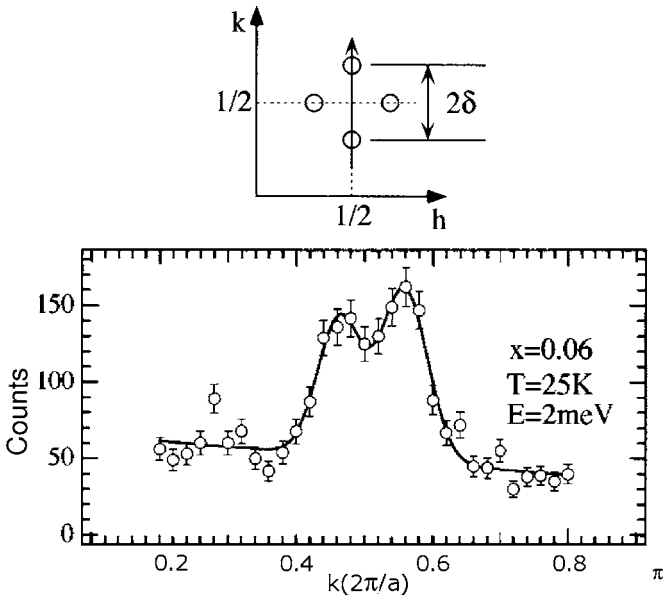

FIG. 5. The existence of low-energy commensurate-incommensurate magnetic excitations in 6%-doped LSCO. From Yamada *et al.* (Ref. 7).

adapted by Rice and co-workers,[8] and has been shown to capture much of the cuprate phenomenology in the appropriate doping range. Recently Fu *et al.* generalized this approach to include the quasiparticle-phonon interaction.[9]

In the following we present the results of pure electronic quasiparticle scattering using a realistic Fermi surface. The quasiparticle dispersion is given by $\epsilon(\mathbf{k})=-2t[\cos(k_x)+\cos(k_y)]+4t'\cos(k_x)\cos(k_y)+4t''[\cos^2(k_x)+\cos^2(k_y)-1]$ where $t'=0.3t$, $t''=-0.1t''$, and $\mu=-0.7t$. These parameters are chosen to produce a Fermi surface similar to those seen in the underdoped cuprates and, in particular, include a nested antinodal region. The qualitative nature of our results remains unchanged as long as the residual quasiparticle interaction is not too weak and the Fermi surface shows a nested antinodal region. The RG flow follows the effective interaction V_Λ for quasiparticles with energy below the cutoff scale Λ as Λ is progressively lowered. The initial quasiparticle interaction is taken to be $U=3t$ at an initial cutoff scale $\Lambda=4t$. In this analysis we only follow the flow of the two-particle scattering vertex in Fig. 8(a), below. Higher-order vertices and self-energy correc-

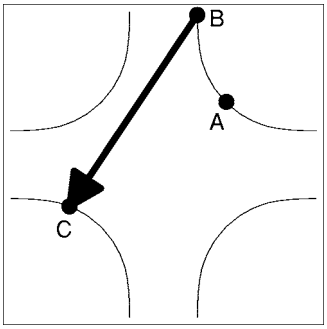

FIG. 6. Schematic illustration of the mechanism of antinodal decoherence.

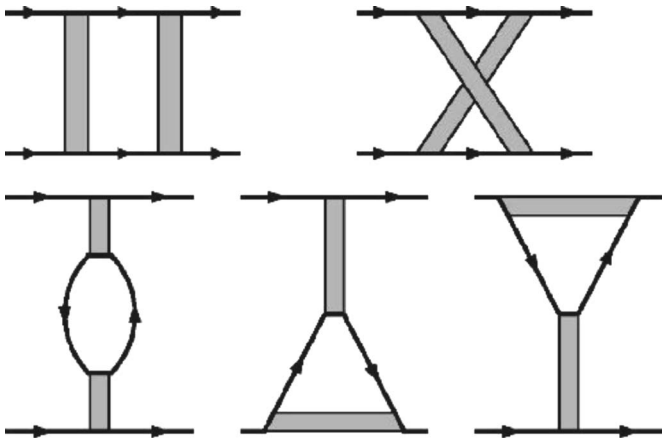

FIG. 7. One-loop diagrams contributing to the RG flow $\partial_\Lambda V_\Lambda$.

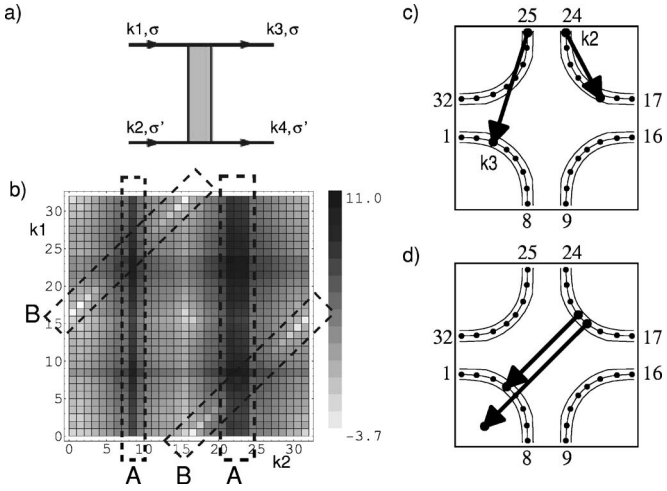

FIG. 8. The renormalized quasiparticle scattering. (a) The quasiparticle scattering vertex. Spin is conserved along solid lines. Each of $\vec{k}_1$, $\vec{k}_2$, $\vec{k}_3$, and $\vec{k}_4$ lies in one of the 32 radial patches of the discretized Brillouin zone. The centers of the intersection between the Fermi surface and the patches are shown as black dots in parts (c) and (d). The patches are indexed counterclockwise from 1 to 32 as shown in the figure. (b) The renormalized quasiparticle scattering amplitudes plotted as a function of $\vec{k}_1$ and $\vec{k}_2$ when $\vec{k}_3$ is fixed at the second dot. The strongest scattering amplitudes are in the boxes labeled *A*. Common among all such strong scattering processes is the momentum transfer $\vec{k}_2-\vec{k}_3\approx(\pi,\pi)$—i.e., the momentum transfer in the spin spin-exchange channel. In addition, all such scattering processes involve electronic excitations in the antinodal region. Aside from the strongest magnetic scatterings, the diagonal boxes labeled *B* correspond to attractive scattering in the *d*-wave Cooper pair channel. (c) An example of the scattering processes that lead to low-energy magnetic fluctuations at momentum $(\pi-\delta,\pi)$. Note that these scattering processes involve antinodal quasiparticle states being scattered antinodal quasiparticle states which would be lower in energy in a system with a *d*-wave gap. (d) An example of the scattering processes that lead to higher-energy spin fluctuations at momentum (π,π). Note that these processes involve quasiparticle states in the nodal direction only.

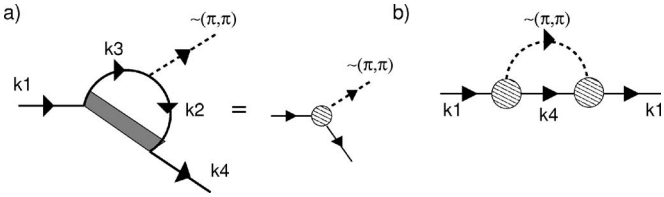

FIG. 9. (a) The interaction of electrons with spin excitations using the strongly renormalized electronic couplings from Fig. 8 as vertices. The dashed line is an outgoing low-energy magnetic excitation. (b) Contribution to the single-particle spectral function which is enhanced by the strongly renormalized couplings through the vertex of part (a). The internal loop corresponds to the multiparticle excitation discussed in the text.

tions are ignored. We include all one-loop contributions to the RG flow $\partial_\Lambda V_\Lambda$, shown in Fig. 7. In each diagram of Fig. 7, one internal line stands for the quasiparticle Green's function

$$G_\Lambda(\mathbf{k},\omega) = \frac{\chi_\Lambda(\mathbf{k})}{i\omega - \epsilon(\mathbf{k}) - \chi_\Lambda(\mathbf{k})\Sigma(\mathbf{k},i\omega)} \tag{1}$$

and the other is given by

$$S_\Lambda(\mathbf{k},\omega) = \frac{\chi'_\Lambda(\mathbf{k})[i\omega - \epsilon(\mathbf{k})]}{[i\omega - \epsilon(\mathbf{k}) - \chi_\Lambda(\mathbf{k})\Sigma(\mathbf{k},i\omega)]^2}, \tag{2}$$

which only has a contribution for $\epsilon(\mathbf{k})$ near the cutoff Λ ($\chi_\Lambda(\mathbf{k}) = 1 - 1/\{\exp[(|\epsilon(\mathbf{k})| - \Lambda)/0.05\Lambda] + 1\}$). The RG flow is computed numerically by discretizing the first Brillouin zone into 32 patches. For more technical details of this calculation, see Ref. 9. The only difference between our flow and the instantaneous flow of Ref. 9 is that our calculation continues the RG flow to a lower scale, determined by when the maximum two-particle scattering vertex reaches a large (arbitrarily set) value.

In Fig. 8(b) the final renormalized scattering amplitude is plotted as a function of the two incoming momenta $\vec{k}_1$ (vertical axis) and $\vec{k}_2$ (horizontal axis) while $\vec{k}_3$ is fixed at the position marked by dot No. 2 in Figs. 8(c) and 8(d). The scattering processes that are dominantly enhanced by the RG flow are those enclosed in the boxes labeled *A*. In these vertical boxes there is a nearly constant momentum transfer $\vec{k}_2 - \vec{k}_3$ in the spin exchange channel. As a result we identify them as being responsible for the spin fluctuations with momenta near (π,π), including "incommensurate" momenta such as $(\pi \pm \delta, \pi)$ and $(\pi, \pi \pm \delta)$. Interestingly, this class of scattering processes involves primarily the antinodal quasiparticle states on the Fermi surface [see Fig. 8(c)]. The fact that only states on the Fermi surface are involved in these scattering processes implies that the corresponding spin fluctuations have low energy. In contrast, all RG-enhanced scattering processes involving only nodal quasiparticles have states off of the Fermi surface. As a result they lead to higher-energy spin fluctuations [see Fig. 8(d)]. This is consistent with the proposal that this type of quasiparticle scattering is responsible for the 41-meV neutron resonance at (π,π).[10] Since these scattering processes must involve high-energy quasiparticles, they do not lead to decoherence of the nodal quasiparticles.

Are the above RG results consistent with the antinodal decoherence mechanism we proposed earlier? Consider the strongest low-energy quasiparticle scattering processes such as Fig. 8(c). Note that while momentum $\vec{k}_2$ lies on the zone boundary, momentum $\vec{k}_3$ lies closer to the nodal region. This is similar to the quasiparticle component of the multiparticle excitation in Fig. 6. Indeed, this scattering process contributes to the vertex describing the scattering of an antinodal excitation into a near-nodal quasiparticle with the emission and absorption of a low-energy commensurate and incommensurate magnetic excitation, as shown in Figs. 9(a) and 9(b). This is precisely the process we invoke in the antinodal decoherence mechanism.

SINGLE-HOLE ARPES AND SPIN WAVES

The ARPES result of insulating cuprates such as $Sr_2CuO_2Cl_2$ (Refs. 1 and 11) has attracted much discussion and attention in the past. For such compounds, the sharp coherent quasiparticle peak [near momenta $(\pm\pi/2, \pm\pi/2)$] is

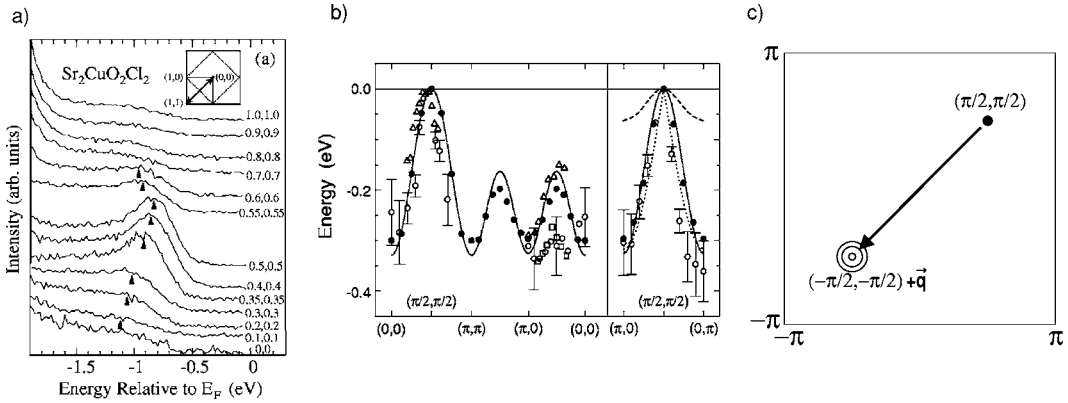

FIG. 10. ARPES spectra of insulating $Sr_2CuO_2Cl_2$, from Damascelli *et al.* (Ref. 1). (a) The broad feature corresponding to nodal excitations near $(\pi/2,\pi/2)$. (b) The dispersion of this feature along two directions. Experimental data points from Refs. 11 are the open symbols. The dispersion is isotropic around $(\pi/2,\pi/2)$. (c) The multiparticle state consisting of a spin wave with momentum $(-\pi,-\pi)+\vec{q}$ and a quasiparticle with momentum $(\pi/2,\pi/2)$ has the same quantum numbers as a photohole at momentum $(-\pi/2,-\pi/2)+\vec{q}$.

replaced by an incoherent broad hump. The hump has an *isotropic* dispersion in the shape of a cone with its tip at momentum $(\pm\pi/2, \pm\pi/2)$. Interestingly, the slope of the dispersion is basically the same as the spin-wave velocity in the antiferromagnet.[12]

This intriguing result has stimulated many theoretical works proposing that the conelike dispersion is due to the spinon of a spin liquid (which is predicted to have an isotropic, conelike dispersion). In view of the decoherence mechanism proposed earlier, here we would like to suggest an alternative, more mundane scenario. We propose that the broad dispersing feature seen in ARPES actually arises from the multiparticle states composed of a quasiparticle at momenta $(\pm\pi/2, \pm\pi/2)$ and a spin wave [see Fig. 10(c)]. The isotropic cone is precisely the spin-wave cone of the antiferromagnet. This is completely analogous to our above proposal that the incoherent antinodal excitations are multiparticle states composed of near-nodal quasiparticles and incommensurate magnetic excitations.

In summary, we propose a mechanism for the decoherence of the antinodal electronic excitations in the underdoped high-temperature superconductors. This mechanism attributes the broad antinodal spectra seen in ARPES to the that of a multiparticle excitation made up of a quasiparticle near the nodes and an incommensurate antiferromagnetic excitation. This point of view is supported by our renormalization group analysis.

We thank J. C. Davis, H. Ding, G.-H. Gweon, C. Honerkamp, A. Lanzara, K. McElroy, K. Shen, Z.-X. Shen, and X.-J. Zhou for useful discussions. This work was supported by the Director, Office of Science, Office of Basic Energy Sciences, Materials Sciences and Engineering Division, of the U.S. Department of Energy under Contract No. DE-AC02-05CH11231 (D.H.L.).

[1] A. Damascelli, Z. Hussain, and Z.-X. Shen, Rev. Mod. Phys. **75**, 473 (2003) and references therein.

[2] X.-J. Zhou, T. Yoshida, D.-H. Lee, W. L. Yang, V. Brouet, F. Zhou, W. X. Ti, J. W. Xiong, Z. X. Zhao, T. Sasagawa, T. Kakeshita, H. Eisaki, S. Uchida, A. Fujimori, Z. Hussain, and Z.-X. Shen, Phys. Rev. Lett. **92**, 187001 (2004).

[3] T. Yoshida, X. J. Zhou, T. Sasagawa, W. L. Yang, P. V. Bogdanov, A. Lanzara, Z. Hussain, T. Mizokawa, A. Fujimori, H. Eisaki, Z.-X. Shen, T. Kakeshita, and S. Uchida, Phys. Rev. Lett. **91**, 027001 (2003).

[4] K. M. Shen, F. Ronning, D. H. Lu, F. Baumberger, N. J. C. Ingle, W. S. Lee, W. Meevasana, Y. Kohsaka, M. Azuma, M. Takano, H. Takagi, and Z.-X. Shen, Science **307**, 901 (2005).

[5] P. W. Anderson, Science **235**, 1196 (1986); G. Kotliar and J. Liu, Phys. Rev. B **38**, 5142 (1988); Y. Suzumura, Y. Hasegawa, and H. Fukuyama, J. Phys. Soc. Jpn. **57**, 2768 (1988); P. W. Anderson, P. A. Lee, M. Randeria, T. M. Rice, N. Trivedi, and F. C. Zhang, J. Phys.: Condens. Matter **16**, R755 (2004); M. Randeria, R. Sensarma, N. Trivedi, and F.-C. Zhang, Phys. Rev. Lett. **95**, 137001 (2005).

[6] J. L. Tallon and J. W. Loram, Physica C **349**, 53 (1998).

[7] K. Yamada, C. H. Lee, K. Kurahashi, J. Wada, S. Wakimoto, S. Ueki, H. Kimura, Y. Endoh, S. Hosoya, G. Shirane, R. J. Birgeneau, M. Greven, M. A. Kastner, and Y. J. Kim, Phys. Rev. B **57**, 6165 (1998).

[8] N. Furukawa, T. M. Rice, and M. Salmhofer, Phys. Rev. Lett. **81**, 3195 (1998); C. Honerkamp, M. Salmhofer, N. Furukawa, and T. M. Rice, Phys. Rev. B **63**, 035109 (2001).

[9] H. C. Fu, C. Honerkamp, and D.-H. Lee, Europhys. Lett. **75**, 146 (2006).

[10] J. Brinckmann and P. A. Lee, Phys. Rev. B **65**, 014502 (2001).

[11] S. La Rosa, I. Vobornik, F. Zwick, H. Berger, M. Grioni, G. Margaritondo, R. J. Kelley, M. Onellion, and A. Chubukov, Phys. Rev. B **56**, R525 (1997); C. Kim, P. J. White, Z.-X. Shen, T. Tohyama, Y. Shibata, S. Maekawa, B. O. Wells, Y. J. Kim, R. J. Birgeneau, and M. A. Kastner, Phys. Rev. Lett. **80**, 4245 (1998); B. O. Wells, Z.-X. Shen, A. Matsuura, D. M. King, M. A. Kastner, M. Greven, and R. J. Bigeneau, *ibid.* **74**, 964 (1995).

[12] M. Greven, R. J. Birgeneau, Y. Endoh, M. A. Kastner, B. Keimer, M. Matsuda, G. Shirane, and T. R. Thurston, Phys. Rev. Lett. **72**, 1096 (1994).